

Delineating Faults beneath Basalt at the Soda Lake Geothermal Field

Lianjie Huang¹, Kai Gao¹, David Li¹, Yingcai Zheng², and Trenton Cladouhos³

¹Los Alamos National Laboratory, MSD452, Los Alamos, NM 87545; ²University of Houston, Department of Earth & Atmospheric Sciences, Houston, Texas 77004; ³Formerly at Cyrq Energy, now at Stoneway Geothermal, Seattle, WA 98103

ljh@lanl.gov

Keywords: Denoise, fault, image noise, machine learning, migration image, migration artifacts, nested residual U-Net, Soda Lake geothermal field

ABSTRACT

Extending geothermal wells beneath basalt at the Soda Lake geothermal field would increase geothermal production because of higher temperatures. Delineating faults beneath the basaltic unit is crucial for optimizing drilling into faults to maximize geothermal production. Because of the large velocity/impedance contrast between basalt and its surrounding formations and complex geologic structures, seismic signals reflected to the surface from geologic formations beneath basalt are very weak and the signal-to-noise ratios are extremely low, resulting in a poor and noisy seismic image. We apply a machine learning method based on nested residual U-Net to reverse-time migration images of a 3D surface seismic data acquired at the Soda Lake geothermal field to reduce image noises and migration artifacts and improve the image resolution, particularly beneath the basaltic unit. We then employ a nested-residual-U-Net fault-detection method to delineate faults on the enhanced migration images. Our procedure improves the reliability of fault detection on seismic migration images. The detected faults could provide valuable information for situating the best drilling locations beneath basalt at the Soda Lake geothermal field to increase geothermal energy production.

1. INTRODUCTION

The Soda Lake geothermal field in the Carson Desert, Nevada has been in production since 1972 (Benoit, 2016). The geothermal field contains a basaltic unit beneath a depth of approximately 500 m (Benoit, 2016; Gao et al., 2021a). Most geothermal production is from geologic formations above the basalt unit. The temperature in the deep region is near 400°F as shown in Figure 1 (Benoit, 2016). Because of higher temperatures in the sub-basalt regions, extending geothermal production wells beneath the basaltic unit would increase geothermal energy production. Therefore, delineating faults beneath the basaltic unit is crucial for optimizing drilling into faults to maximize geothermal production at the Soda Lake geothermal field.

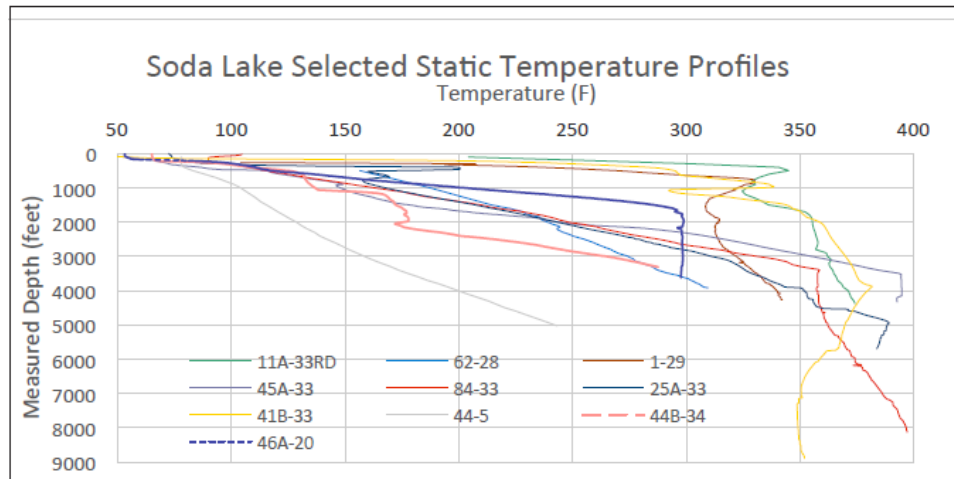


Figure 1: Static temperature profiles at the Soda Lake geothermal field showing the temperature at deeper region is higher than 350°F and near 400°F. (From Benoit, 2016)

A 3D surface seismic dataset was acquired at the Soda Lake geothermal field in 2019. Gao et al. (2021a) performed full-waveform inversion and reverse-time migration and obtained a 3D migration image. Their study showed that obtaining a high-quality, high-resolution subsurface structural image of the Soda Lake geothermal field is a great challenge. The source and receiver distributions of the 3D surface seismic survey depicted in Figure 2 contain many data acquisition gaps in both source and receiver lines. Such data acquisition gaps result in migration artifacts. In addition, the seismic data contain significant noise because of loose ground conditions and complex geologic structures. Because of the large velocity/impedance contrast between basalt and its surrounding formations and complex geologic

structures, seismic reflection signals from geologic formations beneath basalt are very weak, resulting in low signal-to-noise ratios and a poor-quality migration image.

A high-quality, high-resolution migration image is crucial for reliable fault detection. Gao et al. (2021) improved the 3D migration image of the Soda Lake geothermal field using a windowed 2D root-mean-square balancing scheme and a mild nonlinear anisotropic diffusion filter to detect faults using a multiscale connection-fusion U-shaped convolutional neural network (MCFU) (Gao et al., 2022a). However, the nonlinear anisotropic diffusion filter may not be able to remove migration artifacts.

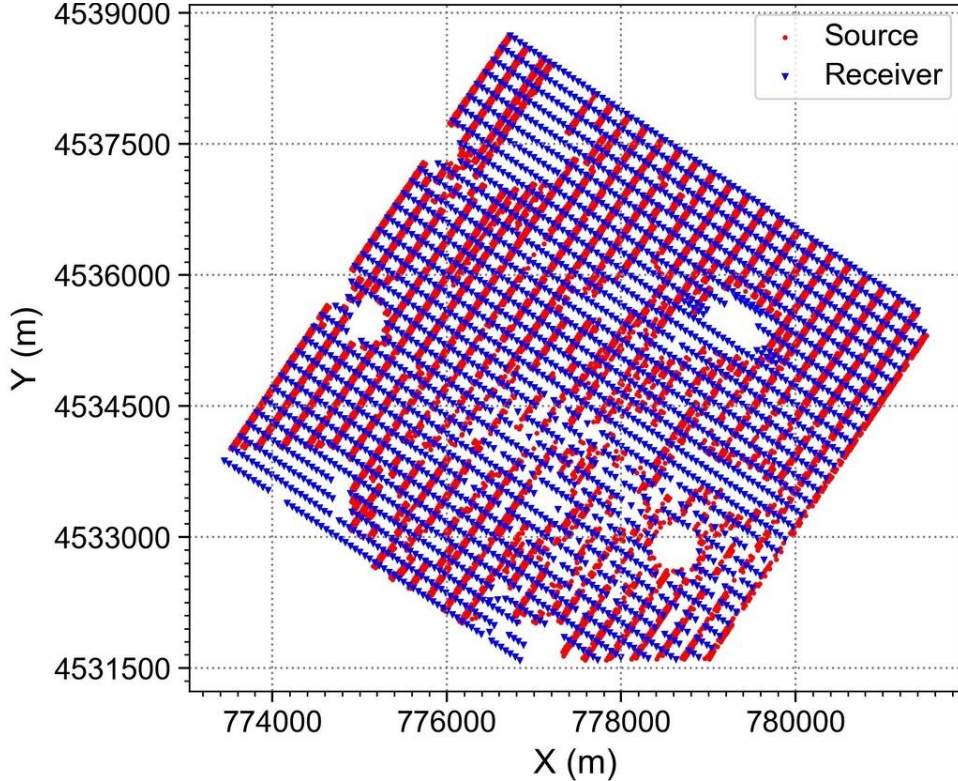


Figure 2: Source and receiver distributions of the 3D surface seismic survey at the Soda Lake geothermal field. The survey contains 8,321 common-shot gathers. Each common-shot gather has a coverage area of up to approximately 3 x 3 km². (From Gao et al., 2021a)

Machine learning is a promising approach to not only denoising migration images, but also removing migration artifacts and improving image resolution (e.g., Wang and Nealon, 2019; Kaur et al., 2020; Li et al., 2021, Wu et al., 2022). Wang and Nealon (2019) trained a 3D supervised deep convolutional neural network (DCNN) on marine seismic images to enhance seismic images and attenuate image noises. Kaur et al. (2020) developed a deep learning method based on generative adversarial network (GAN) to improve image resolution, attenuate image noise, reduce migration artifacts, and enhance reflection image amplitudes. Li et al. (2021) used DCNN to obtain super-resolution migration images and denoise migration images simultaneously. Wu et al. (2022) developed a self-supervised CNN-based approach to attenuating both image noise and migration artifacts simultaneously.

Gao et al. (2022b) developed a nested residual U-Net (NRU) method for automatic fault detection on seismic migration images. We extend the NRU method for reducing noises and migration artifacts and improving image resolution on seismic migration images. We apply the NRU image enhancement method to several 2D slices of the 3D reverse-time migration image from the Soda Lake geothermal field to enhance the image quality and resolution. We then employ the NRU fault detection method to delineate faults on the enhanced migration images. The resulting fault maps could provide useful information to reduce drilling risks and increase geothermal production at the Soda Lake geothermal field.

2. METHODOLOGY

We use a machine learning method to reduce image noise and migration artifacts and improve the spatial resolution of seismic migration images. We then employ a machine learning method to detect faults on the enhanced migration images. Both machine learning methods are based on nested residual U-Net (NRU).

2.1 Improving image quality and resolution using machine learning

Seismic migration images of field surface seismic data often contain significant image noises and migration artifacts because of the uncertainty of subsurface velocity models and imperfect source/receiver distributions. The image resolution of seismic migration images

decreases with depth, and that in the region beneath a basaltic unit of the Soda Lake geothermal field is particularly low. We use the nested residual U-Net (NRU) architecture (Gao et al., 2022b) to reduce noises and migration artifacts and improve image resolution of migration images.

As shown in Figure 3, the NRU at its overall scale consists of a total of five encoders and decoders at three spatial resolution levels: high, medium, and low levels. The high-resolution level consists of encoder 1 and decoder 1, the medium level consists of encoder 2 and decoder 2, and the low level consists of encoder 3. Therefore, in the overall architecture, our NRU is not different from the conventional U-Net. The major difference between NRU and conventional U-Net is that each encoder or decoder in our NRU is an intra-stage subnet, or more precisely, a small-scale residual U-Net, with their respective architectures the same as those in NRU fault detection method (Gao et al., 2022b). These residual U-Nets facilitate the entire architecture to effectively exploit intra-encoder/decoder features, a characteristic that is missing in the conventional U-Net. The overall architecture of our NRU contains another notable difference compared with conventional U-Net. In NRU, after computing a high-resolution image at each of the three spatial resolution levels, the three high-resolution images of different resolutions are then linearly upsampled, concatenated, and convolved through an intermediate convolutional layer to form the final high-quality, high-resolution migration image.

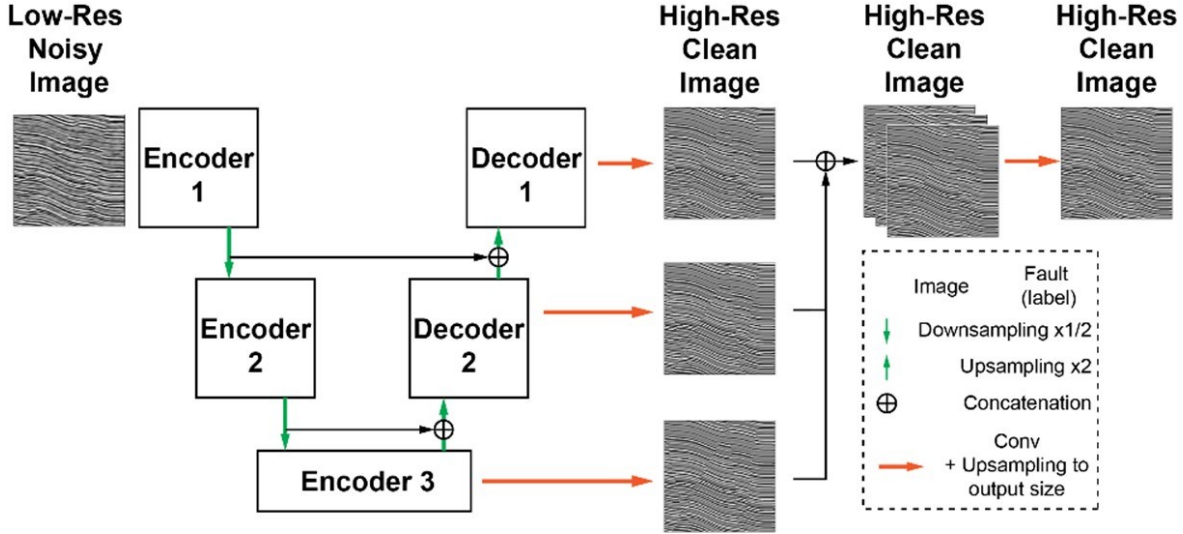


Figure 3: Architecture of NRU image denoising and resolution enhancement. Structures of the encoders and decoders are the same as those in Gao et al. (2022b).

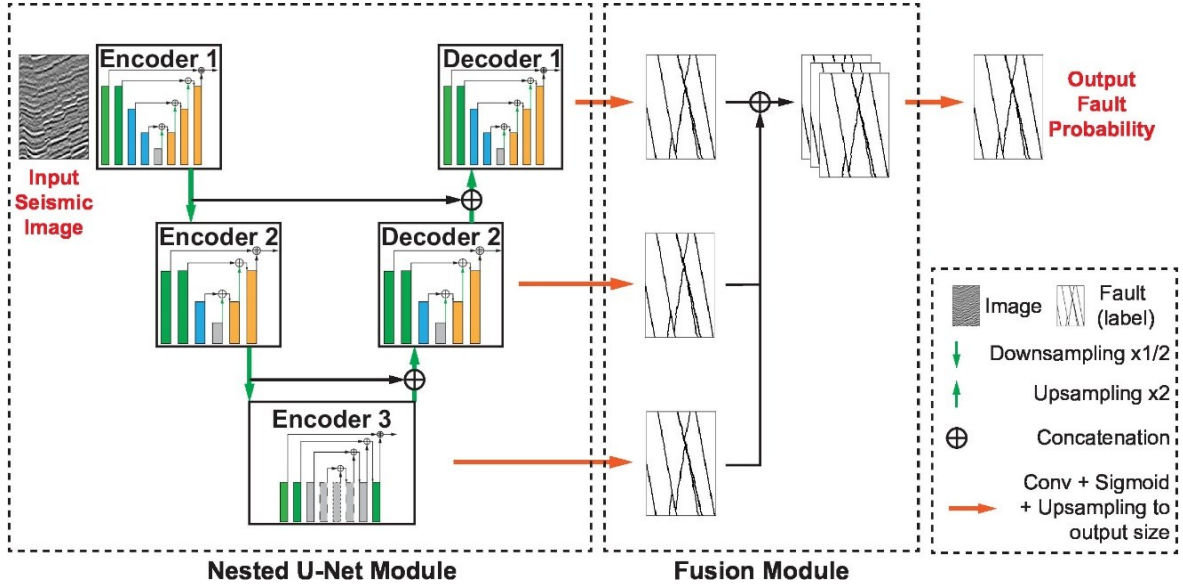


Figure 4: Architecture of NRU fault detection. Each encoder/decoder is an independent residual U-Net. The downsampling or upsampling (denoted by the downward or upward green arrows) use a ratio of 2 x 2 in 2D and 2 x 2 x 2 in 3D. The upsampling operation that generates an output-size layer (denoted by the red horizontal solid-line arrows) is based on bilinear interpolation in 2D and trilinear interpolation in 3D. (From Gao et al., 2022b)

We use an L₂-norm loss function to train the neural network (NN):

$$L = \frac{1}{N} \sum_i^N (y_i^{predict} - y_i^{truth})^2,$$

where N is the number of pixels in an input image or label image.

We use the following procedure to generate a 2D seismic image with or without faults: (1) generate a 1D random reflectivity model; (2) smooth a random-valued array using a Gaussian filter with a random variance to mimic the fluctuation of seismic reflector in the horizontal direction, and assign the generated reflectivity to these deformed seismic reflectors; (3) map these reflectors to a regularly sampled mesh; (4) convolve the reflectivity model with a Ricker or time-integrated Ricker wavelet with a randomly-chosen center frequency; and (5) add a random number of faults (with random dip angles and spatial locations in the 2D image, and shift one of the two blocks with respect to the fault with positive or negative displacement. Using this procedure, we obtain a clean random reflectivity image. To generate the noisy image, we adopt the same procedure but using a Ricker wavelet of lower peak frequency, and at the end of the image generation step, we add random noise to the image with a random level of maximum amplitude. In this manner, we generate a data-label pair. We repeat the process to generate the training and the validation datasets. The training and validation datasets do not overlap to ensure an unbiased assessment of the trained neural network. We then train the NN using an Adam optimizer with an initial learning rate of 0.0001.

2.2 Delineating faults on migration images using machine learning

We use our recently developed nested residual U-Net (NRU) method (Gao et al., 2022b) to delineate faults on the NRU-enhanced migration images and provide useful information to drill beneath the basaltic unit at the Soda Lake geothermal field. This NRU fault detection method employs a nested residual U-shaped convolutional neural network in which each of the encoders and decoders is a residual U-Net, leading to a nested architecture. The input is a seismic migration image, and the output is a fault map resulting from the fusion of three fault maps with low, medium, and high fault resolution. As shown in Figure 4, the NRU fault detection method consists of a total of five encoders and decoders at three spatial resolution levels: high, medium, and low. The high-resolution level consists of encoder 1 and decoder 1, the medium level consists of encoder 2 and decoder 2, and the low level consists of encoder 3. The overall architecture of the NRU fault detection in Figure 4 is the same as that for NRU image enhancement in Figure 3, except that the output is either a fault map in NRU fault detection or an enhanced migration image in NRU image enhancement.

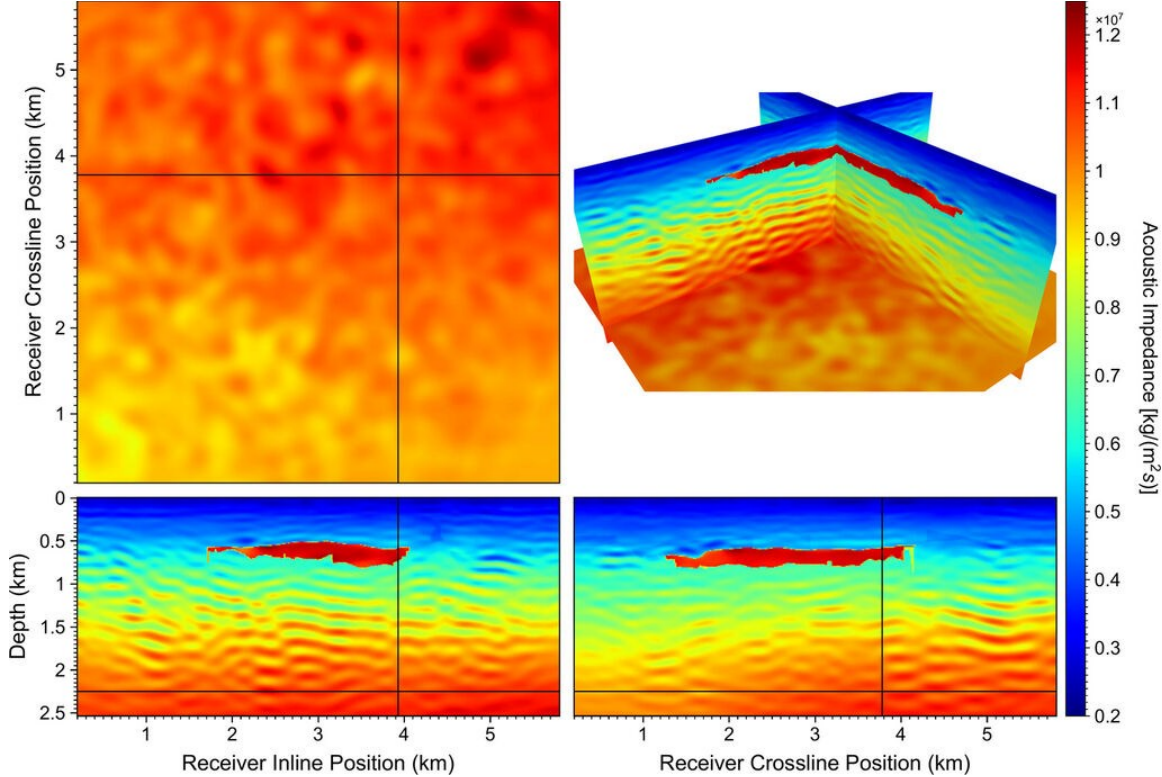


Figure 5: Slices and a 3D view of the acoustic impedance model obtained using full-waveform inversion of the 3D surface seismic data acquired at the Soda Lake geothermal field where the red region beneath the depth of approximately 500 m is a basaltic unit. (Gao et al., 2021a)

3. RESULTS

The Soda Lake geothermal field contains a basaltic unit beneath the depth of approximately 500 m, as shown in Figure 5 of the 3D acoustic impedance model obtained using full-waveform inversion of the 3D surface seismic data (Gao et al., 2021a). Because of the large velocity/impedance contrast between basalt and its surrounding formations, seismic signals reflected to the surface from geologic formations beneath the basaltic unit are very weak and the signal-to-noise ratios are extremely low, resulting in a poor and noisy seismic image. Gao et al. (2021a) employed a windowed 2D root-mean-square balancing scheme to balance the image amplitudes from the shallow region to the deep region.

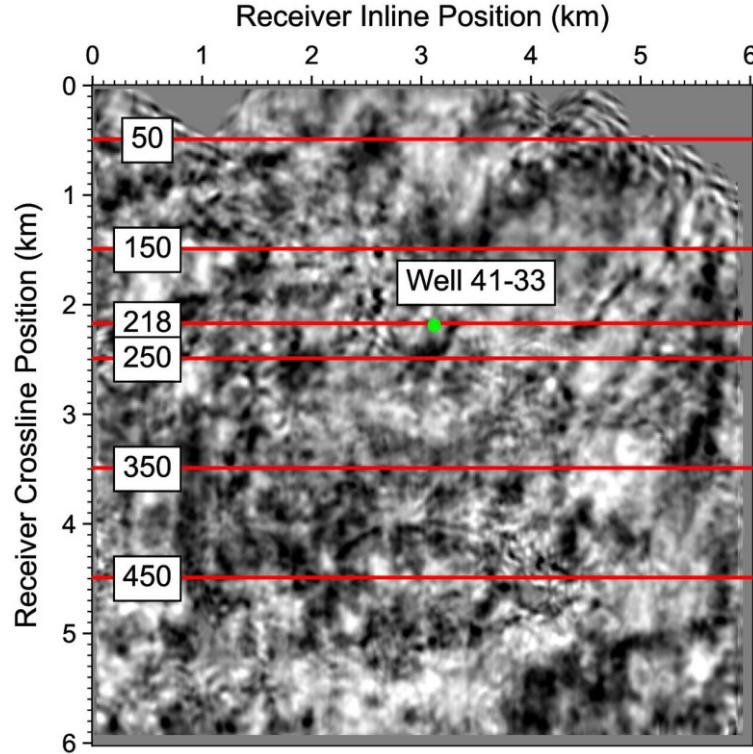


Figure 6: The red lines are the locations of six 2D vertical (depth) slices of migration images extracted from the 3D reverse-time migration image of the Soda Lake geothermal field for this study. Well 41-33 is a geothermal production well from a steam zone at depth of approximately 242-303 m (800-1000 ft). The background image is a horizontal slice at the depth of 300 m around the steam zone.

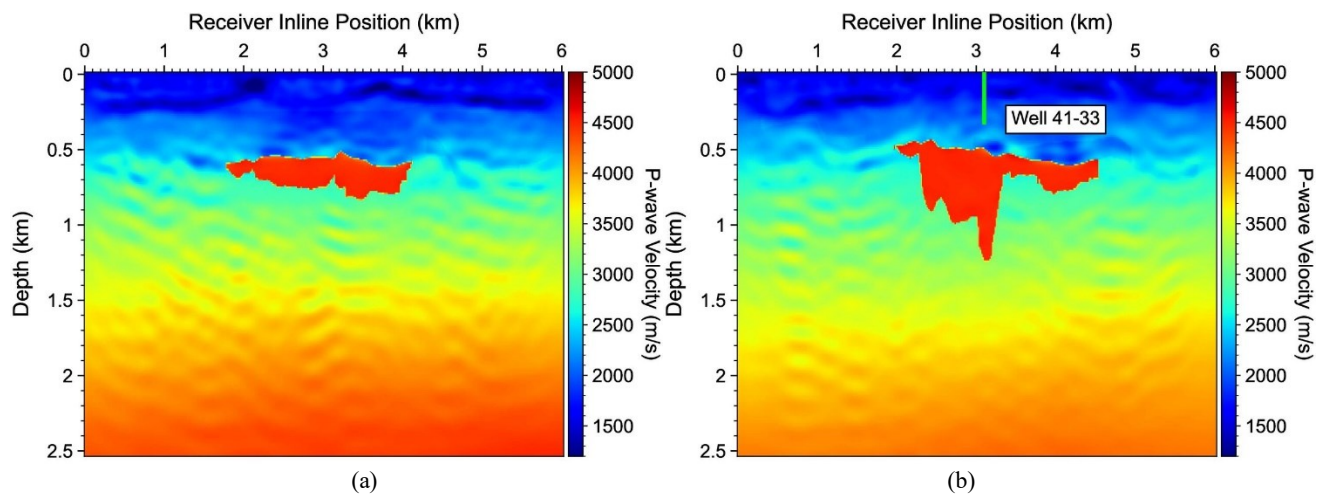


Figure 7: The velocity models of the 3D full-waveform inversion result along (a) Line 350 and (b) Line 218 as shown in Figure 6. The red region at depth beneath approximately 500 m in each panel is a basaltic unit. The green vertical line in (b) is Well 41-33, a geothermal production well from a steam zone at depth of approximately 242-303 m (800-1000 ft).

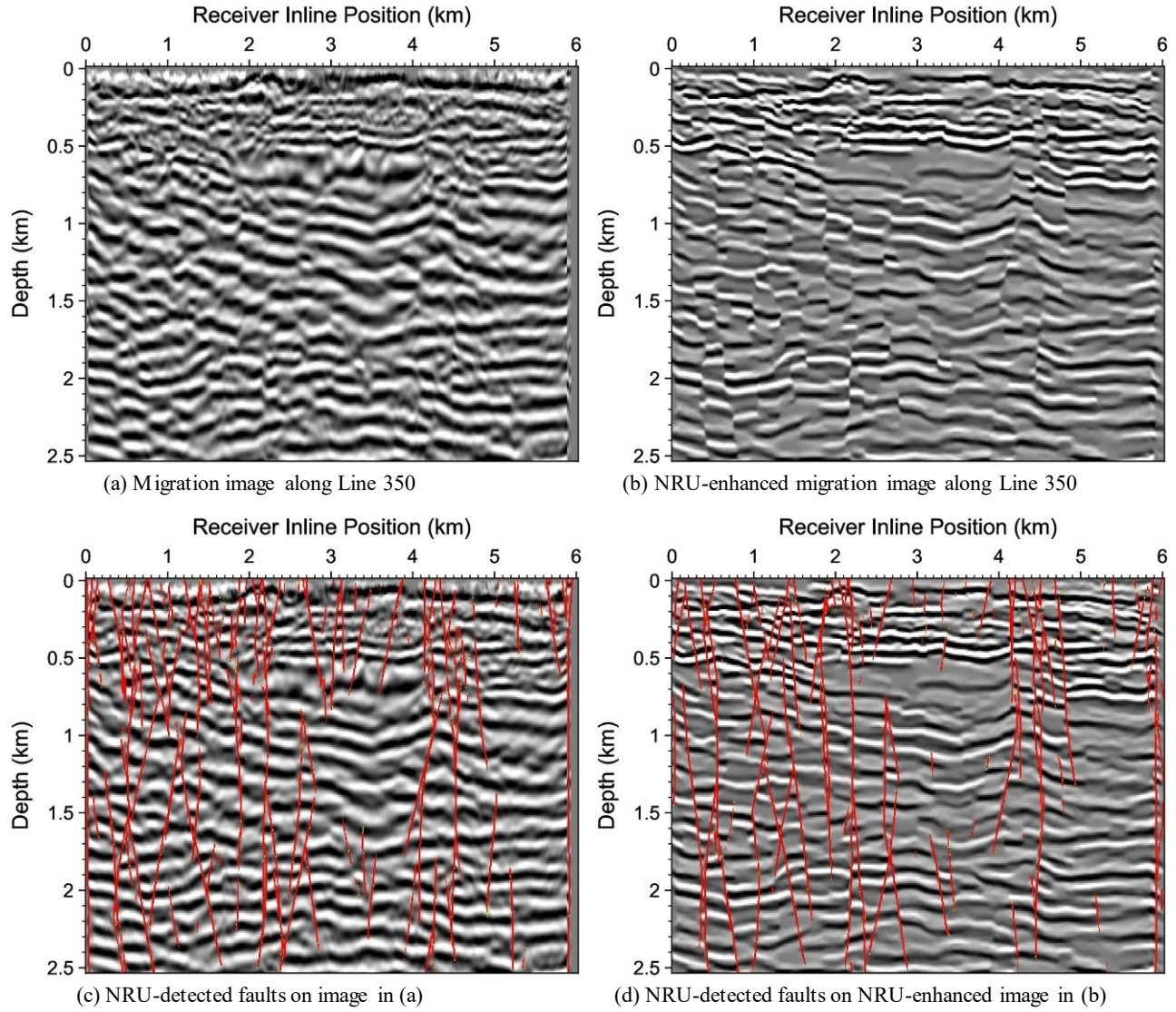


Figure 8: Reverse-time migration image along Line 350 in (a) contains significant image noise and migration artifacts, which are mostly eliminated in the NRU-enhanced migration image in (b). Comparison between (c) faults detected on the original reverse-time migration image and (d) those detected on the NRU-enhanced image using the NRU fault detection method.

We extract six 2D vertical (depth) slices from the 3D reverse-time migration image of the Soda Lake geothermal field (Gao et al., 2021a) for this study. Figure 6 shows the locations of these six 2D slices where the background image is a horizontal slice of the 3D image at a depth of 300 m around a steam zone located at depth of approximately 242-303 m (800-1000 ft). Figure 7 shows that the 2D vertical sections along Line 350 and 218 contain basalt in the red regions. Line 218 passes through Well 41-33, a geothermal production well producing energy from a steam zone. The geothermal company is exploring to increase energy production from steam zones.

We first apply our NRU image enhancement method to each 2D slice of the reverse-time migration image to obtain a migration image with considerably reduced image noise and migration artifacts and substantially enhanced image resolution. As an example, we only show our results for Lines 350 and 218. The original reverse-time migration images in Figure 8(a) and Figure 9(a) contain balanced image amplitudes from the shallow region to the deep region after applying a windowed 2D root-mean-square balancing. Nevertheless, NRU fault detection on these images is still challenging as depicted in Figure 8(c) and Figure 9(c). The image quality and resolution of NRU-enhanced images in Figure 8(b) and Figure 9(b) are much better than those in Figure 8(a) and Figure 9(a). The NRU image enhancement removes most image noises and migration artifacts, and substantially increases the image resolution. NRU fault detection on these images produces much more reliable fault maps as shown in Figure 8(d) and Figure 9(d). As depicted in Figure 9(d), the steam production well interests with a fault. Our NRU-detected faults on NRU-enhanced migration images could provide valuable information for situating the best drilling locations beneath basalt at the Soda Lake geothermal field.

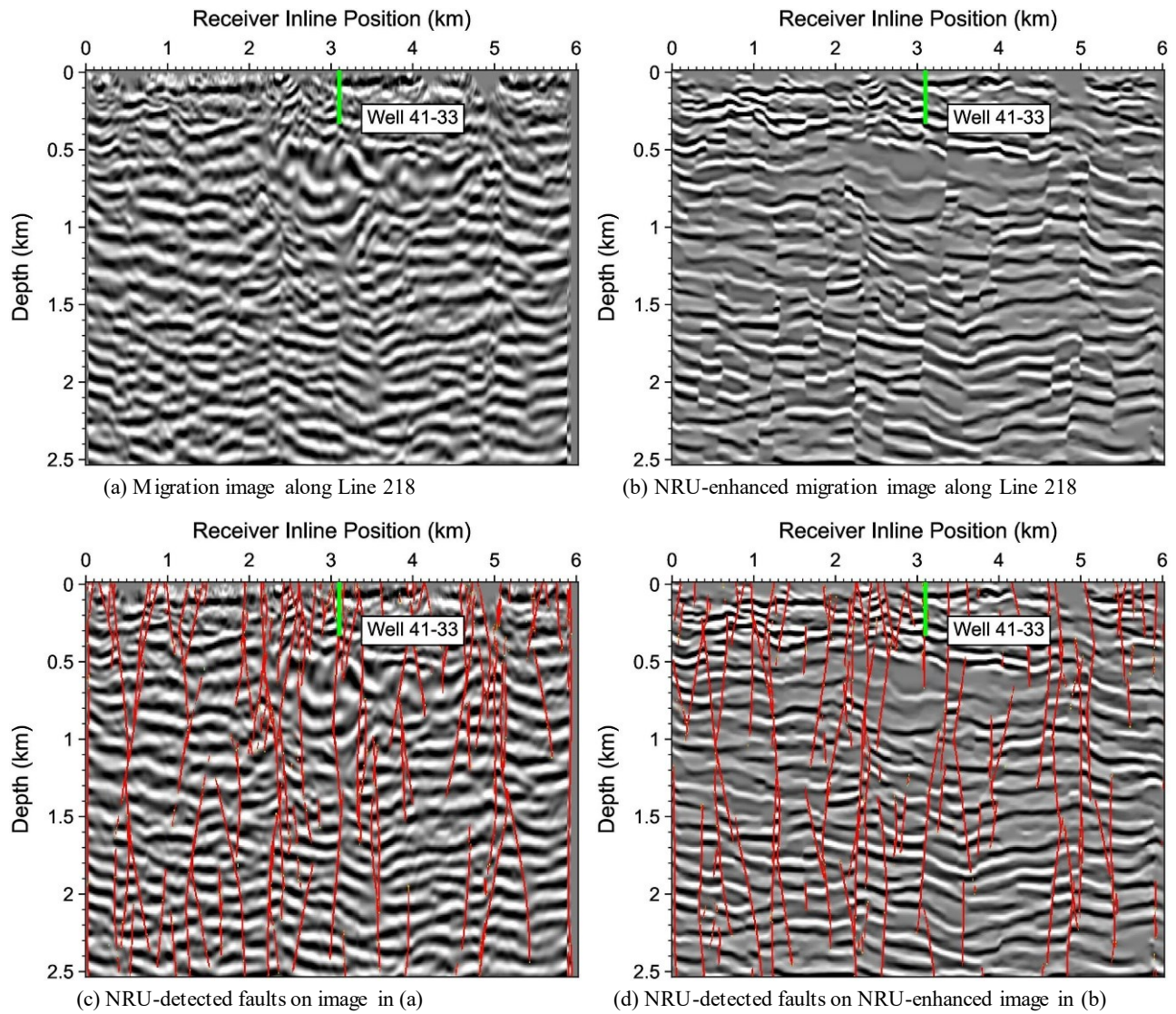


Figure 9: Reverse-time migration image along Line 218 in (a) contains significant image noise and migration artifacts, which are mostly eliminated in the NRU-enhanced migration image in (b). Comparison between (c) faults detected on the original reverse-time migration image and (d) those detected on the NRU-enhanced image using the NRU fault detection method. The green line is a geothermal production well from a steam zone at depth of approximately 242-303 m (800-1000 ft) above the basaltic unit.

4. CONCLUSIONS

We have enhanced the quality and resolution of seismic migration images from the Soda Lake geothermal field using a nested residual U-Net. The high-quality, high-resolution migration images enable reliable fault detection using machine learning. We have employed a nested residual U-Net fault detection to delineate faults on the enhanced migration images and produced reliable fault maps above and beneath basalt at the Soda Lake geothermal field. These fault maps could provide valuable information for situating the best drilling locations beneath basalt to increase geothermal production at the Soda Lake geothermal plant.

ACKNOWLEDGMENTS

The work was supported by the Geothermal Technologies Office of the U.S. Department of Energy (DOE) under award No. DE-EE0008764, a joint project between the University of Houston and Los Alamos National Laboratory (LANL). LANL is operated by Triad National Security, LLC, for the National Nuclear Security Administration (NNSA) of U.S. DOE under Contract No. 89233218CNA000001. This research used resources provided by the LANL Institutional Computing Program, which is supported by the U.S. DOE NNSA under Contract No. 89233218CNA000001.

REFERENCES

Benoit, D., 2016, Soda Lake Geothermal Field Case History 1972 to 2016, GRC Transactions, Vol. 40, 523-534.

Gao, K., L. Huang, and T. Cladouhos, 2021a, Three-dimensional seismic characterization and imaging of the Soda Lake geothermal field, *Geothermics* 90, 101996.

Gao, K., L. Huang, R. Lin, H. Hu, Y. Zheng, T. Cladouhos, 2021b, Delineating faults at the Soda Lake geothermal field using machine learning, 2021, *Proceedings of the 46th Workshop on Geothermal Reservoir Engineering*.

Gao, K., L. Huang, Y. Zheng, R. Lin, H. Hu, T. Cladouhos, 2022a, Automatic fault detection on seismic images using a multiscale attention convolutional neural network, *Geophysics*, 87, N13-N29.

Gao, K., L. Huang, and Y. Zheng, 2022b, Fault Detection on Seismic Structural Images Using a Nested Residual U-Net: IEEE Transactions on Geoscience and Remote Sensing, 60, 1-15, 2022, doi: 10.1109/TGRS.2021.3073840.

Kaur, H. Kaur, N. Pham, and S. Fomel, 2020, Improving the resolution of migrated images by approximating the inverse Hessian using deep learning, *Geophysics*, 85(4), WA173-WA183, doi: 10.1190/geo2019-0315.1.

Li, J., X. Wu, and Z. Hu, 2021, Deep Learning for Simultaneous Seismic Image Super-Resolution and Denoising: IEEE Transactions on Geoscience and Remote Sensing, 60, 5901611, doi: 10.1109/TGRS.2021.3057857.

Wang, E. and J. Nealon, 2019, Applying machine learning to 3D seismic image denoising and enhancement, *Interpretation* (2019) 7 (3): SE131–SE139.

Wu, H., B. Zhang, and N. Liu, 2022, Self-adaptive denoising net: Self-supervised learning for seismic migration artifacts and random noise attenuation, *Journal of Petroleum Science and Engineering*, 214, 110431.